

# Free Lunch for Gait Recognition: A Novel Relation Descriptor

Jilong Wang<sup>1,2,4</sup>, Saihui Hou<sup>3,4</sup>, Yan Huang<sup>2</sup>, Chunshui Cao<sup>4</sup>, Xu Liu<sup>4</sup>, Yongzhen Huang<sup>3,4</sup>, Liang Wang<sup>2\*</sup>

<sup>1</sup>University of Science and Technology of China

<sup>2</sup>Institute of Automation, Chinese Academy of Sciences

<sup>3</sup>Beijing Normal University

<sup>4</sup>WATRIX.AI

jilongw@mail.ustc.edu.cn, {yhuang, liangwang}@nlpr.ia.ac.cn

{housaihui, huangyongzhen}@bnu.edu.cn, {chunshui.cao, xu.liu}@watrix.ai

## Abstract

Gait recognition is to seek correct matches for query individuals by their unique walking patterns at a long distance. However, current methods focus solely on individual gait features, disregarding inter-personal relationships. In this paper, we reconsider gait representation, asserting that gait is not just an aggregation of individual features, but also the relationships among different subjects' gait features once reference gaits are established. From this perspective, we redefine classifier weights as reference-anchored gaits, allowing each person's gait to be described by their relationship with these references. In our work, we call this novel descriptor **Relationship Descriptor (RD)**. This Relationship Descriptor offers two benefits: emphasizing meaningful features and enhancing robustness. To be specific, The normalized dot product between gait features and classifier weights signifies a similarity relation, where each dimension indicates the similarity between the test sample and each training ID's gait prototype, respectively. Despite its potential, the direct use of relationship descriptors poses dimensionality challenges since the dimension of RD depends on the training set's identity count. To address this, we propose a Farthest Anchored gaits Selection algorithm and a dimension reduction method to boost gait recognition performance. Our method can be built on top of off-the-shelf pre-trained classification-based models without extra parameters. We show that RD achieves higher recognition performance than directly using extracted features. We evaluate the effectiveness of our method on the popular GREW, Gait3D, CASIA-B, and OU-MVLP, showing that our method consistently outperforms the baselines and achieves state-of-the-art performances.

## 1. Introduction

Gait recognition is a biometric application that aims at identifying people at a long distance by their unique walking patterns, even without the explicit cooperation of subjects [26]. As an identification task in vision, the essential goal of it is to learn the distinctive and invariant representations from the physical and behavioral human walking characteristics. With the boom of deep learning, gait recognition has achieved great progress [6, 10, 11, 27, 33], yielding impressive results on public datasets.

Reappraising an established pipeline of gait recognition [10, 16, 19, 31], prior work typically involves a frame-by-frame feature extractor and usually utilizes a classifier for identity classification. Specifically, *Feature Extractor* firstly obtains a unique gait feature from spatial-temporal characteristics of individual walking sequences; Then, *Classifier* [10, 20] learns the mapping from the gait feature to specific categories, thereby achieving the task of gait classification. However, gait recognition is an open-set recognition task, which means all the test identities are unseen at the training stage. Hence, the classifier for training set classification loses its significance for test identities and is usually discarded at the inference stage. However, the classifier typically occupies the majority of the network's weights especially when the number of training classes is large. A natural question would arise: **whether the classifier for the training set is really useless for inference?**

In this work, we draw wisdom from human beings: **human nature is the ensemble of social relations** instead of abstraction inherent in every single individual [17]. We assume that gait goes beyond just an aggregation of individual features; it can also be expressed through the relationships with the gait features of others. These relationships may involve aspects of similarity, dissimilarity, common traits, etc., reflecting patterns and variations of gait within a population. For example, with several preselected different in-

\*Corresponding Author

dividuals' gaits as anchored references, each new person's gait can be described as the differences/similarities with these anchored reference gaits.

Motivated by it, we rethink the role of the classifier by reinterpreting its weights as the well-defined gait prototype for each person in the training set, essentially serving as anchored gaits. Hence, a person's gait can be re-expressed by the relations between the extracted feature and the well-defined anchored gaits. To be specific, the normalized dot product of gait features and anchored gaits represents similarities [14], constructing a new descriptor of test identities, namely, Relation Descriptor (RD). Since the weights in the classifier denote the well-defined gait feature in the training set, RD can be seen as a projection of gait features on these meaningful semantic weights. Thereby, RD brings two natural benefits: 1) emphasizing meaningful features instead of noise and 2) more robust and generalizable ability. Moreover, the proposed descriptor can be obtained without any extra costs.

However, directly employing relationship descriptors poses the challenge of dimension expansion or shrinking, as the number of anchored gaits in the classifier is dependent on the count of training identities. For instance, the dimension of classifier weights is 20000 in GREW [39], thus the dimension of the final relation descriptor would be expanded to 20000. When there are too many anchor gaits, the dimension of the relationship descriptor usually exceeds that of the original embedding, bringing augmented storage costs and impracticality for real-world deployment. What's more, not all identities in the training set are needed since there may be many similar identity prototypes. This will inevitably result in many redundant relationships. On the other hand, when there are too few anchor gaits, the patterns and variations of gait within this group would be less varied, thus reducing the discrimination of expression.

To overcome these drawbacks, we assume that the most discriminative combination of anchored weights in the latent space should be the one with the largest spanning space, *i.e.*, the maximum divergence. For the problem of **dimension expansion**, we introduce a novel farthest weights sampling algorithm to meticulously select the most discriminative set of anchored gaits. Then, if the number of sampling bases is still larger than the embedding dimension, a Singular Value Decomposition (SVD) would be adopted to reduce the dimensions of the bases matrix without losing essential information. For the problem of **dimension shrinking**, we propose an orthogonal regulation loss for better classifier training, which increases the distances among anchored gaits. We rigorously evaluate our proposed approach on established benchmark datasets including GREW [39], Gait3D [38], CASIA-B [34], and OU-MVLP [28], consistently demonstrating its superiority over conventional baseline methods.

To summarize, the contributions of our work can be outlined in three aspects:

- We propose a novel descriptor for gait recognition, capturing not only individual features but also relationships among well-trained gait representations, which enhances recognition performance without extra costs.
- We address dimension expansion and shrinking by farthest weights sampling algorithm and orthogonal regulation, improving efficiency and discrimination.
- We evaluate the effectiveness of our proposed method on four popular datasets, and the extensive experimental results demonstrate the superior performance of our approach.

## 2. Related Work

### 2.1. Gait Recognition

Gait recognition aims to identify people by their unique representation of their gait characteristics. According to their type of inputs, current works can be roughly grouped into model-based and appearance-based categories. Model-based methods [1, 4, 18, 37] pay attention to modeling the static structures and dynamic relations among key points of the human body. Appearance-based [6, 11, 15, 16, 19, 27] approaches methods directly obtain spatial-temporal features from binary gait silhouettes. No matter what kind of input it is, previous works mainly focus on spatiotemporal pattern extraction, multi-scale feature learning, stronger network architectures, and representation learning. Thanks to the contributions of prior work, a typical pipeline of gait recognition has been established. It primarily consists of four components: 1) a spatial-temporal feature extractor (CNN [6, 7, 10, 11, 19, 31], Transformer [9, 32], GCN [12, 29], and *et al.*), 2) a temporal pooling module (MaxPooling [6], Mean-Pooling [27], GeM [19], and *et al.*), 3) a multi-scale module (HPP [6], attention [7, 8], body parsing, and *et al.*), 4) and metric learning loss functions (Triplet Loss [25], Cross-entropy Loss [36], and *et al.*).

However, without exception, previous works have emphasized extracting discriminative individual-specific gait features from gait sequences, thereby overlooking the relationships among different gait sequences. In this work, we propose a novel perspective that a person's gait characteristics can also be described by the relationships between their own gait and other anchor gaits. Furthermore, we highlight the importance of the classifier that is usually discarded in prior work during inference stage.

### 2.2. Open-set Recognition

Gait recognition is also an open-set recognition task where the identities in test set are unseen during the training stage. Yet, it differs from typical open-set recognition

in several aspects. Open-set recognition requires rejecting inputs from unknown classes [23], which minimizes open space risk. The data labeled as ‘unknown’ class should be far from the ‘known’ training classes in the latent space while maintaining the classification accuracy on the known classes [23]. In the area of open-set recognition, researchers have noticed that the logits of the classifier can be used to reject unknown classes, thereby highlighting the importance of the logits. OpenMax [3] models all known classes by their logits as a single cluster and uses a Weibull distribution to re-calibrate softmax scores according to the distance between input and other cluster centers. Several following works [13, 21, 22, 24] propose many mechanisms to improve the feature representation for distance-based measures, such as data augmentation or introducing an ‘other’ class. Recent works [5, 30] find that a good close-set classifier can directly boost the performance of open-set recognition, which prompts a reconsideration of the role of classifiers.

However, techniques proposed in open-set recognition mainly enlarge the distance between ‘unknown’ and ‘known’ classes which is a different goal in gait recognition. In our work, we advocate the discriminative capacity of logits.

### 3. Our Approach

In this work, we revisit the role of classifiers in the testing phase of gait recognition and thus propose a new gait descriptor. We find the well-trained weights in the classifier can be regarded as anchored gaits, and the relationship between the gait feature and the set of anchored gaits can be used as a discriminative descriptor. In this section, we first introduce our new pipeline of relation-based gait recognition. Then, we will thoroughly explain the proposed descriptor and how to construct it. What’s more, we introduce our proposed mechanisms, including farthest anchored selection, SVD dimension reduction, and orthogonal Regulation Loss, in order to solve challenges brought by relationship descriptors.

#### 3.1. Pipeline

We follow a typical gait recognition procedure [10, 19] during the training phase. Given a dataset with data-label pairs  $\mathcal{D} = \{(x_i, y_i)\}$  where  $x_i$  denotes a gait sequence and  $y_i \in C$  indicates the class label of  $x_i$ .  $\mathcal{D}$  will be divided into training set  $D_{train}$  and test set  $D_{test}$ , where  $C_{train} \cap C_{test} = \emptyset$ . The  $\Omega$  is a feature extractor that embeds the gait sequences into a  $d$ -dimensional latent space, where  $z_i = \Omega(x_i)$  is the extracted representation. The goal of training  $\Omega$  on  $D_{train}$  is to learn a discriminative transformation from  $x_i$  to  $z_i \in \mathbb{R}^d$ , satisfying that the intra-class variations are smaller than inter-class differences.

In order to get a more discriminative  $\Omega$ , a common practice combines triplet loss [25] and cross-entropy loss [36]

as objective functions. A BNNeck classifier [20] with a weights matrix  $W_c \in \mathbb{R}^{d \times C}$  would be introduced during the training stage for the classification task. In our work, we adopt a cosine similarity classifier [14]. The  $r_i \in \mathbb{R}^C$  indicates the normalized dot product results of  $z_i$  with all identities’ gait prototypes, where the larger  $r_i^j$  is, the more similar  $z_i$  and  $W_c^j$  are.

Unlike prior work, we keep the classifier during the inference stage. In order to obtain more discriminative anchored references, the Farthest Anchor Selection(FAS) algorithm is adopted to select a good subset of reference gait features from the  $W_c$ . Next, we further reduce the dimension of this selected set by SVD. In the end, we calculate the relation descriptor  $r_i$  between the testing gaits and the set of anchored gaits for the final individual identification.

#### 3.2. A Novel Relationship Descriptor

We now introduce the core idea of our paper: gait goes beyond just an aggregation of individual features; it can also be expressed through the relationships with the gait features of others.

To be specific, gait is usually seen as a unique walking pattern for each individual, influenced by various factors including body structure, posture, stride length, and more. Previous works run identification on this level, assuming each dimension of  $z_i$  refers to unique individual features and the Euclidean distances between these features indicate the similarity between different identities’ gaits. It can be formulated as

$$dist(z_a, z_b) = \sqrt{\sum_i^d (z_a^i - z_b^i)^2} \quad (1)$$

However, gait can be also expressed by comparing the relationships between the gait features of different individuals, which involves aspects of similarity, dissimilarity, and common traits. For example, person  $I$ ’s gait can be described as 0.2 of *anchored gait* (AG) 1, 0.7 of AG2, 0.01 of AG3, -0.5 of AG4, and so on. Here we use cosine similarity for relationship measurement. As a result, a novel descriptor of person  $I$  can be  $r_1 = [0.2, 0.7, 0.01, -0.5, \dots]$ , which denotes the relationship between other anchored persons. We call this descriptor as **relationship descriptor**. Based on the new descriptor, Euclidean distances can be also defined as

$$dist(r_a, r_b) = \sqrt{\sum_i^{|AG|} (r_a^i - r_b^i)^2} \quad (2)$$

where  $|AG|$  is the number of anchored gaits.

Based on the above discussion, it is easy to notice that the discriminative ability of the relationship descriptor heavily relies on the set of anchored gaits. The higher the diversity of patterns and variations within the anchored gaits group is, the stronger the discrimination capability of the relationship descriptor is. To find a good set of anchored

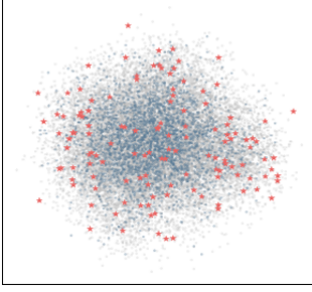


Figure 1. PCA visualization of training data (gray),  $W_c$  (dark blue) in classifier, and  $W_{c,s}$  (red) selected by FAS.

gaits, we set our sights on the *cosine similarity classifier*. We know the Cross-entropy loss would minimize the negative log-probability of an input’s ground truth class, thereby, the weights in the classifier would encapsulate specific gait representations only tied to each identity in the training set. Hence, the weight can be seen as a well-defined anchored gait that represents a discriminative feature of a specific identity. Their normalized dot product with test gait features represents similarity, signifying the relationship descriptors of test identities. It can be formulated as

$$r_i = \frac{W_c^T \cdot z_i}{\|W_c\| * \|z_i\|} \quad (3)$$

where the  $\|W_c\|$  is the 2-norm of  $W_c$  along the  $d$  dimension. And the Eq. 2 can be rewritten as

$$d(r_a, r_b) = \sqrt{\sum_j^C \frac{W_{c,j}^T}{\|W_{c,j}^T\|} \cdot \left( \frac{z_a}{\|z_a\|} - \frac{z_b}{\|z_b\|} \right)} \quad (4)$$

The proposed descriptor can be obtained without any extra costs, and the knowledge hidden behind the classifier be further unearthed.

**Compared to EigenFace and FisherFace.** The EigenFace [35] shows that principal component analysis (PCA) could be used to search for a collection of base features, called eigenfaces. All faces in the training set can be linearly represented by these eigenfaces, in other words, all face images can be described by the ”proportions” of all the eigenfaces. FisherFace [2] shares similar ideas but takes advantage of linear discriminant analysis (LDA) to search for more discriminative bases. Our idea inspired by these works, the anchored gaits are regarded as semantic bases in the latent space, which is learned by a non-linear model with higher discriminative ability. The normalized dot product between  $z_i$  and  $W_c$  can be seen as a projection on these anchored gaits.

---

#### Algorithm 1 Pseudo-code of FAS in a PyTorch-like style.

---

```
# W_c : weight matrix, (Cxd)
# W_cs: selected weight, (Nxd)
# cdist(): matrix-wise L2 distance

dist = cdist(W_c, W_c.t())
# the farthest weight from all others
farthest = dist.sum(-1).argmax()
W_cs[0] = W[farthest]
# remove the selected basis from W
W.remove(farthest)

for i in range(1,N):
    dist = cdist(W_cs.mean(dim=1), W.t())
    farthest = dist.sum(-1).argmax()
    W_cs[i] = W[farthest]
    W.remove(farthest)
```

---

### 3.3. Anchored Gait Selection And Dimension Reduction

As we discussed above, the anchored gaits can be seen as a set of semantic bases in the latent space, but, the number of bases relies on the number of training identities. When training on a large-scale dataset, the dimension of  $W_c$  is inevitably expanding, incurring augmented storage costs and redundant information. Therefore, the combination of anchored gaits should be carefully selected.

**What is a good combination of anchored gaits?** The latent space is a manifold determined by the training data, and the class center can be seen as bases that span the manifold. Borrowing the idea from EigenFace, we know that each training feature can be expressed by these bases. Thus, in order to maintain the discriminative ability, the manifold spanned by the combination of selected anchored gaits needs to be as consistent as possible with the original manifold. Additionally, when the  $C > d$ , there are many linearly related bases in the classifier which can be removed.

Based on the above discussion, we assume that the most discriminative combination of anchored gaits should be the one with the largest spanning space, *i.e.*, the maximum within-divergence.

**Farthest Anchor Selection.** Given weights in the classifier  $\{W_{c,1}, W_{c,2}, \dots, W_{c,C}\}$ , we use iterative farthest anchor selection (FAS) to choose a combination of  $N$  weights  $\{W_{c,s1}, W_{c,s2}, \dots, W_{c,sN}\}$  as anchored gaits, where the  $W_{c,sj}$  is the farthest weights from the barycenter of the set  $\{W_{c,s1}, W_{c,s2}, \dots, W_{c,sj-1}\}$ . The final selected weights are denoted by  $W_{c,s} \in \mathbb{R}^{d \times N}$ . The distances are computed by Euclidean distances. FAS is a greedy algorithm described in Algorithm 1 and a visualization of this process is shown in Figure 3.

The internal mechanism of FAS is based on the assumption that the farthest weight from the selected weights contains the most different semantic information, thus, it is good for increasing the diversity of the combination an-



chored gaits. Compared to the original  $W_c$ , the  $W_{c,s}$  collects the discriminative anchored gaits and removes redundant ones.

**Towards to further dimension reduction.** Even though the FAS would filter out some useless weight, the number of anchored gaits is usually larger than the original embeddings' dimension. Thus, we propose to use the Singular Value Decomposition (SVD) to further reduce the dimensions.

SVD is performed on the selected weight matrix to decompose the feature:

$$W_{c,s} = U\Sigma V^T \quad (5)$$

where  $\Sigma \in \mathbb{R}^{d \times N}$  rectangular diagonal singular value matrix,  $U \in \mathbb{R}^{d \times d}$  and  $V \in \mathbb{R}^{N \times N}$  are left and right orthogonal singular vector matrices, respectively. Then we select only top- $k$  weights from the  $W_{c,s}$  by

$$W_{c,r} = U[:, :k] \Sigma[:, :k] \quad (6)$$

where  $W_{c,r}$  is the dimension-reduced anchored gaits.

### 3.4. Orthogonal Regulation Loss

When there are only a few identities in the training stage, especially  $C < d$ , the classifier is easily over-fitted. Thus, the class weights of it would be less discriminative. To overcome this limitation, we propose an orthogonal regulation loss (ORL) to minimize the correlation between different identity prototypes, which can be formulated as

$$L_{ORL} = ||W_c^T W_c - I||_1 \quad (7)$$

where  $I \in \mathbb{R}^{C \times C}$ .

ORL is inspired by the above finding that weights with maximum within-divergence are more discriminative. And ORL is only used in small datasets with few identities.

## 4. Experiments

### 4.1. Datasets

**GREW** [39]. GREW is the largest outdoor dataset, containing 26,345 subjects with 128,671 sequences captured from 882 cameras. GREW provides various types of gait sequences, such as silhouettes, optical flow, 2D/3D human poses, and *et al.*. According to its official partition, GREW is divided into three subsets, *i.e.*, the training set with 20,000 subjects, the validation set with 345 subjects, and the test set with 6,000 subjects.

**Gait3D** [38]. Gait3D is an in-the-wild dataset, containing 4000 subjects with over 25,000 sequences captured from 39 cameras. To facilitate a fair comparison with other algorithms, Gait3D provides an official protocol that 3000 subjects are used for training while the remaining 1000 subjects are for test. For the test set, the probe set is constructed by

randomly selecting one sequence from a subject, while the other sequences are regarded as the gallery set.

**OU-MVLP** [28]. The OU-MVLP is the largest indoor gait dataset under a fully controlled environment. It includes 10,307 subjects under normal walking conditions and 14 views uniformly distributed between  $[0^\circ, 90^\circ]$  and  $[180^\circ, 270^\circ]$ . In addition, each view embodies 2 sequences, thus, each subject has  $2 \times 14 = 28$  sequences. In our work, we adopt the widely-used protocol that 5153 subjects are used for training and the rest are taken for the test. At the test phase, the sequences with index #01 are treated as galleries while the rest are regarded as probes.

**CASIA-B** [34]. It is one of the most popular gait datasets, which contains 124 subjects from 11 view angles ( $0^\circ, 18^\circ, 36^\circ, 54^\circ, 72^\circ, 90^\circ, 108^\circ, 126^\circ, 144^\circ, 162^\circ$  and  $180^\circ$ ). For each subject under each view, there are 10 sequences under 3 walking conditions, namely normal walking (NM, the first 6 sequences), carrying bags (BG, the other 2 sequences), and wearing a coat or jacket (CL, the last 2 sequences). In other words, each subject has  $(6 + 2 + 2) \times 11 = 110$  gait sequences. There is no official partition of training and test in CASIA-B. Thus, for fairness, our work follows the popular partition constructed by [6]. To be specific, the first 74 subjects are used for training and the remaining 50 subjects are reserved for the test.

### 4.2. Implementation Details

we utilize GaitBase [10] as our main baseline on Gait3D, GREW, and OU-MVLP. And GaitGL [19] as baseline on CASIA-B. The number of  $N$  in FAS is set to 74, 1024, 2048, and 8192 in the above four datasets, respectively. The  $k$  in SVD is set to as the same as embedding dimension  $d$ . ORL is only used to train the model on CASIA-B.

Most experiments are directly using the pre-trained weights of these models. Whereas, we also reproduce some methods in our experiments. For these reproduced models [6, 11], they all use the following settings.

Frames size is set to  $64 \times 44$ . The optimizer is SGD with an initial learning rate set to 0.1. The momentum and weight decay are set to 0.9 and  $5e-4$ , respectively. The objective functions are Batch-All Triplet loss and Cross-entropy loss, and the coefficients are all set to 1 in our experiments. We implement our method on the OpenGait codebase. For CASIA-B and Gait3D, we train the model for 50k iterations with a batch size of (8, 16) and (32, 4) respectively. The learning rate will drop by 10 times at 20k, 30k, and 40k iterations. For OU-MVLP, we train the model for 120k iterations with a batch size of (32, 8). The learning rate will drop by 10 times at 60k, 80k, and 100k iterations. For GREW, we train the model for 180k iterations with a batch size of (32, 4). The learning rate will drop by 10 times at 80k, 120k, and 150k iterations.

Table 1. Rank-1 accuracy (%), Rank-5 accuracy (%), Rank-10 accuracy (%), and Rank-20 accuracy (%) on the GREW dataset.

Methods	Rank-1	Rank-5	Rank-10	Rank-20
PoseGait	0.2	1.0	2.2	4.3
GaitGraph	1.3	3.5	5.1	7.5
GEINet	6.8	13.4	17.0	21.0
TS-CNN	13.6	24.6	30.2	37.0
GaitSet	46.3	63.6	70.3	76.8
GaitPart	44.0	60.7	67.3	73.5
GaitGL	47.3	63.6	69.3	74.2
MGN	44.5	61.3	67.7	72.7
CSTL	50.6	65.9	71.9	76.9
MTSGait	55.3	71.3	76.9	81.6
GaitBase	60.1	75.7	80.5	84.4
GaitBase+ours	<b>65.5</b>	<b>78.7</b>	<b>83.3</b>	<b>86.3</b>

### 4.3. Performance Comparison

**GREW.** We compare the performance of the proposed method with several gait recognition methods[] on the GREW dataset and show experimental results in Tab. 1. GREW is collected under an unconstrained condition, thus it contains lots of unpredictable external covariants, such as occlusion and bad segmentation. As a result, gait sequences in the test set may be encoded by some unseen covariant that further produces meaningless gait representation. From Tab. 1, we can see the gait recognition methods that perform well on indoor datasets meet a large performance degradation. It shows the gait representations encoded by only individual features are not robust enough. By replacing our relation descriptor incorporating FAS and SVD, our method elevate the accuracy of the state-of-the-art GaitBase[] by 5.4%, 3.0%, 2.8%, and 1.9% on Rank-1, Rank-5, rank-10, and rank-20, respectively. It is worth noting that our method adds no extra parameters and the dimension of the final gait representation is the same as the original GaitBase. The experimental results indicate that the relation descriptor is more discriminative and robust in real-world scenarios.

**Gait3D.**Gait3D is also an unconstrained dataset. Hence, some competing gait recognition methods on fully-controlled indoor datasets cannot perform well on it. The comparison of prevailing competing methods is illustrated in Tab. 2, demonstrating that our proposed method exhibits superior performance compared to previous methods by a considerable margin. Since our method utilizes the relationship between test gait and well-defined anchored gaits, it will be less affected by unseen external covariants. As a result, our method outperforms all prevailing methods and can boost the performance of GaitBase by 5.4%, 6.7%, and 5.8% on Rank-1, mAP, and mINP, respectively.

**OU-MVLP and CASIA-B.** Since both OU-MVLP and CASIA-B are collected in a fully-constrained laboratory

Table 2. Rank-1 accuracy(%), mAP, and mINP comparison on Gait3D. The bold number denotes the best performances.

Method	Venue	Gait3D		
		Rank-1	mAP	mINP
PoseGait	PR20	0.2	0.5	0.3
GaitGraph	ICIP21	6.3	5.2	2.4
GaitSet	AAAI19	36.7	30.0	17.3
GaitPart	CVPR20	28.2	21.6	12.4
GLN	ECCV20	31.4	24.7	13.6
GaitGL	ICCV21	29.7	22.3	13.3
CSTL	ICCV21	11.7	5.6	2.6
SMPLGait	CVPR22	46.3	37.2	22.2
GaitBase	CVPR23	64.6	55.2	30.4
GaitBase+ours	-	<b>70.1</b>	<b>61.9</b>	<b>36.2</b>

Table 3. Ablation study on relationship descriptors (RD), Farthest Anchor Selection (FAS), and Orthogonal Regulation Loss (ORL) on CASIA-B and Gait3D.

	RD	FAS	ORL	CASIA-B	Gait3D
				Mean Acc. $\uparrow$	Rank-1 Acc. $\uparrow$
#1				91.8	64.6
#2	✓			90.6 $\downarrow-1.2$	68.8 $\uparrow+2.2$
#3	✓	✓		N/A	<b>70.1</b> $\uparrow+5.5$
#4	✓		✓	<b>92.5</b> $\uparrow+0.7$	N/A

Table 4. Model agnostic results on Gait3D dataset.

Rank-1 Acc.	Methods			
	GaitSet	GaitPart	GaitGL	GaitBase
Baseline	36.7	28.2	29.7	64.6
w. Ours	42.5 $\uparrow+5.8$	38.0 $\uparrow+9.8$	37.1 $\uparrow+7.4$	70.1 $\uparrow+5.5$

environment, their training and testing sets possess nearly identical covariates. The effects of covariates can be well eliminated during the training stage. Hence, directly using individual gait features as representation can achieve promising accuracy. However, we find our method can still boost the baseline performance on these two datasets, especially when the number of training identities is large. On the OU-MVLP, our method boosts GaitBase accuracy across all viewpoints by using relation descriptors computed on 2500 anchored gaits. On the CASIA-B, our methods improve the average accuracy of GaitGL by 0.7%. Notably, the dimension of the relation descriptors on CASIA-B is 74 since only 74 identities are in the training set. Thus, our method achieves higher accuracy with fewer feature dimensions. The experiments have demonstrated that relationship descriptors exhibit discriminative capability com-

Table 5. Averaged rank-1 accuracy (%) on OU-MVLP, excluding identical-view cases.

Methods	Prove View															Mean
	0°	15°	30°	45°	60°	75°	90°	180°	195°	210°	225°	240°	225°	270°		
GEINet	23.2	38.1	48.0	51.8	47.5	48.1	43.8	27.3	37.9	46.8	49.9	45.9	45.7	41.0	42.5	
GaitSet	79.3	87.9	80.0	90.1	88.0	88.7	87.7	81.8	86.5	89.0	89.2	87.2	87.6	86.2	87.1	
GaitPrart	82.6	88.9	90.8	91.0	89.7	89.9	89.5	85.2	88.1	90.0	90.1	89.0	89.1	88.2	88.7	
GLN	83.8	90.0	91.0	91.2	90.3	90.0	89.4	85.3	89.1	90.5	90.6	89.6	89.3	88.5	89.2	
GaitGL	84.9	90.2	91.1	91.5	91.1	90.8	90.3	88.5	88.6	90.3	90.4	89.6	89.5	88.8	89.7	
GaitBase	85.6	90.7	91.5	91.8	90.9	90.7	90.2	87.5	90.1	90.8	91.1	90.2	90.0	89.5	90.0	
GaitBase+ours	<b>87.3</b>	<b>91.4</b>	<b>91.9</b>	<b>92.1</b>	<b>91.4</b>	<b>91.2</b>	<b>90.8</b>	<b>89.0</b>	<b>90.7</b>	<b>91.2</b>	<b>91.3</b>	<b>90.7</b>	<b>90.6</b>	<b>90.1</b>	<b>90.7</b>	

Table 6. Averaged rank-1 accuracy (%) on CASIA-B, excluding identical-view cases.

Gallery NM#1-4		Prove View											
Probe		0°	18°	36°	54°	72°	90°	108°	126°	144°	162°	180°	Mean
NM#5-6	GaitSet	90.8	97.9	99.4	96.9	93.6	91.7	95.0	97.8	98.9	96.8	85.8	95.0
	GaitPart	94.1	98.6	<b>99.3</b>	<b>98.5</b>	94.0	92.3	95.9	98.4	99.2	97.8	90.4	96.2
	MT3D	95.7	98.2	99.0	97.5	95.1	93.9	96.1	98.6	99.2	98.2	92.0	96.7
	GaitBase	-	-	-	-	-	-	-	-	-	-	-	<b>97.6</b>
	GaitGL	<b>96.0</b>	98.3	99.0	97.9	<b>96.9</b>	<b>95.4</b>	97.0	<b>98.9</b>	<b>99.3</b>	<b>98.8</b>	94.0	97.4
	GaitGL+ours	95.5	<b>98.6</b>	98.9	97.9	96.5	94.8	<b>97.5</b>	98.8	98.8	98.3	<b>94.2</b>	97.3
BG#1-2	GaitSet	83.8	91.2	91.8	88.8	83.3	81.0	84.1	90.0	82.2	84.4	79.0	87.2
	GaitPart	89.1	94.8	96.7	95.1	88.3	84.9	89.0	93.5	96.1	93.8	85.8	91.5
	MT3D	91.0	95.4	97.5	94.2	92.3	86.9	91.2	95.6	97.3	96.4	86.6	93
	GaitBase	-	-	-	-	-	-	-	-	-	-	-	94.0
	GaitGL	92.6	<b>96.6</b>	<b>96.8</b>	95.5	<b>93.5</b>	<b>89.3</b>	92.2	96.5	98.2	<b>96.9</b>	<b>91.5</b>	94.5
	GaitGL+ours	<b>94.0</b>	96.3	96.6	<b>95.8</b>	93.4	88.8	<b>92.8</b>	<b>97.1</b>	<b>98.6</b>	96.8	89.2	<b>94.5</b>
CL#1-2	GaitSet	61.4	75.4	80.7	77.3	72.1	70.1	71.5	73.5	73.5	68.4	50.0	70.4
	GaitPart	70.7	85.5	86.9	83.3	77.1	72.5	76.9	82.2	83.8	80.2	66.5	78.7
	GaitBase	-	-	-	-	-	-	-	-	-	-	-	77.4
	MT3D	76.0	87.6	89.8	85.0	81.2	75.7	81.0	84.5	85.4	82.2	68.1	81.5
	GaitGL	76.6	90.0	90.3	87.1	84.5	79.0	84.1	87.0	87.3	<b>84.4</b>	69.5	83.6
	GaitGL+ours	<b>77.6</b>	<b>90.6</b>	<b>92.2</b>	<b>89.0</b>	<b>85.0</b>	<b>79.9</b>	<b>87.0</b>	<b>89.1</b>	<b>89.6</b>	82.3	<b>70.9</b>	<b>84.9</b>

parable to or higher than individual gait features. Furthermore, as the number of candidate anchor gaits increases, the performance of the relationship descriptors improves.

#### 4.4. Ablation Study

In this subsection, we provide the ablation study of each component in our method on the CASIA-B and Gait3D.

**Analysis of RD, FAS, and ORL.** The ablation result is illustrated in Tab. 3. Note that the farthest anchor selection is only employed for on datasets where the number of identities  $C$  in the training set exceeds the output dimension  $d$ . In contrast, ORL is only applied on datasets where  $C < d$ . Here is the analysis: 1) from experiment #2, RD improves the baseline by 2.2% on Gait3D but degrades the performance on CASIA-B by 1.2% due to fewer anchored gaits; 2) Comparing #4 with #2, adding ORL to generate more

separate anchored gaits brings improvement on CASIA-B, which shows the importance of anchored gaits; 3) Comparing #4 with #2, the selected combination of anchored gaits can further improve the recognition accuracy, which demonstrates that not all weights in the classifier are discriminative enough and our FAS would produce a better combination. Overall, the ablation result verifies the effectiveness of our proposed methods.

**Analysis of model agnostic results.** As shown in Tab. 4, we conduct experiments on Gait3D with four popular methods, including GaitSet, GaitPart, GaitGL, and GaitBase. Since GaitSet and GaitPart don't use cross-entropy loss, we train an extra cosine similarity classifier for them. Then for these four methods, we adopt FAS to select 1024 anchored gaits from their classifiers and then adopt SVD to keep the dimension of the relation descriptor the same as their original

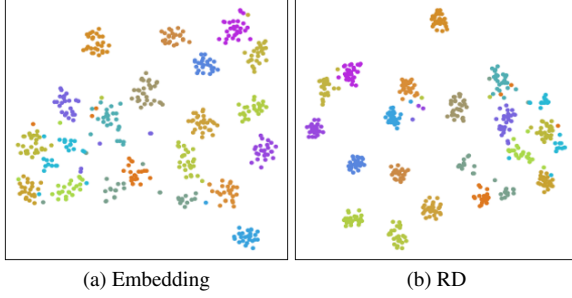


Figure 2. T-SNE visualization on Gait3D test set with randomly selected 20 classes. One color denotes a class.

embeddings. The results show that the proposed method can improve performance regardless of the baseline backbones or network structures. The model agnostic property further verifies the superior discriminative capacity of the relation descriptor.

**Analysis of the value  $N$  in FAS.** As we mentioned above, not all weights in the classifier contribute to better recognition performance. From Fig. 3b, we can conclude that: first, the performance of relation descriptor relies on the pre-selected anchored gaits; second, it is important to note that selecting too few or all of the weights doesn't necessarily lead to performance improvement, where the curve first rises and then falls as  $N$  is increased. Compared to random selection, FAS can bring consistent performance improvement, which proves our assumption that the most discriminative combination of anchored gaits should be the one with the largest spanning space.

**Analysis of the relationship between classifier convergence and accuracy.** The relation descriptor depends on the well-defined weights in the classifier, which is based on the assumption that each weight represents a typical gait representation. The cross-entropy loss requires separating the weights of different identities. Hence, the weights in a classifier with better convergence can better represent distinct gait features, leading to superior results. This phenomenon can be observed in Fig. 3a.

#### 4.5. Visualization

In this section, we visualize the feature distribution of models' original embeddings and RD on Gait3D test set with 20 randomly selected classes. By comparing Figs. 2a and 2b, we can observe that the intra-class variation is further reduced and the inter-class distance is hence enlarged by our relation descriptor. The visualization demonstrates that RD is more discriminative representation.

Furthermore, we visualize the anchored gaits selection results of FAS on the GaitBase in the Gait3D training set. As shown in Fig. 1, the gray circles are the feature of all training sequences, the dark blue circles indicate all weights in the classifier, and the red star denotes the se-

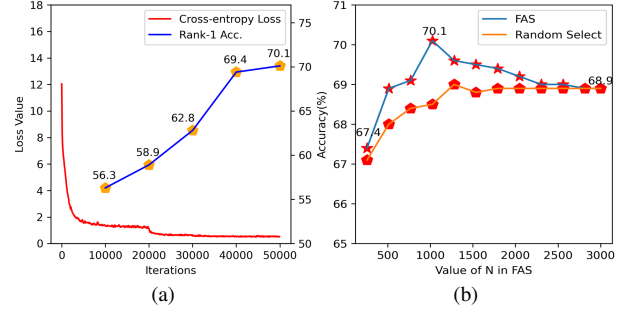


Figure 3. (a) The cross-entropy loss and accuracy curves of GaitBase on Gait3D. (b) Ablation study on the number of selected anchored gaits in FAS on Gait3D.

lected weights by FAS. We can observe that the dark blue weights are mostly concentrated in the center, while the selected weights are mainly distributed on the periphery. It shows that when the number of training identities is large, it inevitably contains numerous similar weights that contain similar gait representations. Thus, our FAS would filter out similar weights and select the discriminative ones.

## 5. Conclusion

In this paper, we propose a novel Relationship Descriptor for gait recognition. The descriptor captures not only individual features but also the relationships between the test sample and predefined anchor samples. To construct the relationship descriptor, we reconsider the role of the classifier by regarding its weights as predefined anchor gait examples. We prove a new way to leverage knowledge in the classifier's weights which is usually discarded in previous work. Despite its potential, we also notice dimensionality challenges caused by using RD. To address them, we carefully design FAS and ORL to maintain the number of dimensions and further boost the recognition performance. Overall, we hope these new insights on representing gait by relative expressions could spur further research in gait community.

## References

- [1] Gunawan Ariyanto and Mark S. Nixon. Model-based 3d gait biometrics. In *2011 International Joint Conference on Biometrics (IJCB)*, pages 1–7, 2011. 2
- [2] Peter N. Belhumeur, Joao P Hespanha, and David J. Kriegman. Eigenfaces vs. fisherfaces: Recognition using class specific linear projection. *IEEE Transactions on pattern analysis and machine intelligence*, 19(7):711–720, 1997. 4
- [3] Abhijit Bendale and Terrance E Boulton. Towards open set deep networks. In *Proceedings of the IEEE conference on computer vision and pattern recognition*, pages 1563–1572, 2016. 3
- [4] R. Bodor, A. Drenner, D. Fehr, O. Masoud, and N. Papanikolopoulos. View-independent human motion classifi-



- cation using image-based reconstruction. *Image Vision Comput.*, 27(8):1194–1206, jul 2009. [2](#)
- [5] Jun Cen, Di Luan, Shiwei Zhang, Yixuan Pei, Yingya Zhang, Deli Zhao, Shaojie Shen, and Qifeng Chen. The devil is in the wrongly-classified samples: Towards unified open-set recognition. *arXiv preprint arXiv:2302.04002*, 2023. [3](#)
- [6] Hanqing Chao, Kun Wang, Yiwei He, Junping Zhang, and Jianfeng Feng. GaitSet: Cross-view gait recognition through utilizing gait as a deep set. *IEEE transactions on pattern analysis and machine intelligence*, 44(7):3467–3478, 2021. [1](#), [2](#), [5](#)
- [7] Huanzhang Dou, Pengyi Zhang, Wei Su, Yunlong Yu, and Xi Li. Metagait: Learning to learn an omni sample adaptive representation for gait recognition. In *European Conference on Computer Vision*, pages 357–374. Springer, 2022. [2](#)
- [8] Huanzhang Dou, Pengyi Zhang, Wei Su, Yunlong Yu, Yining Lin, and Xi Li. Gaitgci: Generative counterfactual intervention for gait recognition. In *Proceedings of the IEEE/CVF Conference on Computer Vision and Pattern Recognition*, pages 5578–5588, 2023. [2](#)
- [9] Chao Fan, Saihui Hou, Yongzhen Huang, and Shiqi Yu. Exploring deep models for practical gait recognition. *arXiv preprint arXiv:2303.03301*, 2023. [2](#)
- [10] Chao Fan, Junhao Liang, Chuanfu Shen, Saihui Hou, Yongzhen Huang, and Shiqi Yu. Opengait: Revisiting gait recognition towards better practicality. In *Proceedings of the IEEE/CVF Conference on Computer Vision and Pattern Recognition (CVPR)*, pages 9707–9716, June 2023. [1](#), [2](#), [3](#), [5](#)
- [11] Chao Fan, Yunjie Peng, Chunshui Cao, Xu Liu, Saihui Hou, Jiannan Chi, Yongzhen Huang, Qing Li, and Zhiqiang He. GaitPart: Temporal part-based model for gait recognition. In *2020 IEEE/CVF Conference on Computer Vision and Pattern Recognition (CVPR)*, pages 14213–14221, 2020. [1](#), [2](#), [5](#)
- [12] Yang Fu, Shibe Meng, Saihui Hou, Xuecai Hu, and Yongzhen Huang. Gpgait: Generalized pose-based gait recognition. *arXiv preprint arXiv:2303.05234*, 2023. [2](#)
- [13] ZongYuan Ge, Sergey Demyanov, Zetao Chen, and Rahil Garnavi. Generative openmax for multi-class open set classification. *arXiv preprint arXiv:1707.07418*, 2017. [3](#)
- [14] Spyros Gidaris and Nikos Komodakis. Dynamic few-shot visual learning without forgetting. In *Proceedings of the IEEE conference on computer vision and pattern recognition*, pages 4367–4375, 2018. [2](#), [3](#)
- [15] J. Han and Bir Bhanu. Individual recognition using gait energy image. *IEEE Transactions on Pattern Analysis and Machine Intelligence*, 28(2):316–322, 2006. [2](#)
- [16] Saihui Hou, Chunshui Cao, Xu Liu, and Yongzhen Huang. Gait lateral network: Learning discriminative and compact representations for gait recognition. In *Computer Vision - ECCV 2020: 16th European Conference, Glasgow, UK, August 23-28, 2020, Proceedings, Part IX*, pages 382–398, Berlin, Heidelberg, 2020. Springer-Verlag. [1](#), [2](#)
- [17] Alison M Jaggard. *Feminist politics and human nature*. Rowman & Littlefield, 1983. [1](#)
- [18] Worapan Kusakunniran, Qiang Wu, Hongdong Li, and Jian Zhang. Multiple views gait recognition using view transformation model based on optimized gait energy image. In *2009 IEEE 12th International Conference on Computer Vision Workshops, ICCV Workshops*, pages 1058–1064, 2009. [2](#)
- [19] Beibei Lin, Shunli Zhang, and Xin Yu. Gait recognition via effective global-local feature representation and local temporal aggregation. In *Proceedings of the IEEE/CVF International Conference on Computer Vision (ICCV)*, pages 14648–14656, October 2021. [1](#), [2](#), [3](#), [5](#)
- [20] Hao Luo, Wei Jiang, Youzhi Gu, Fuxu Liu, Xingyu Liao, Shenqi Lai, and Jianyang Gu. A strong baseline and batch normalization neck for deep person re-identification. *IEEE Transactions on Multimedia*, 22(10):2597–2609, 2019. [1](#), [3](#)
- [21] Dimity Miller, Niko Sunderhauf, Michael Milford, and Feras Dayoub. Class anchor clustering: A loss for distance-based open set recognition. In *Proceedings of the IEEE/CVF Winter Conference on Applications of Computer Vision*, pages 3570–3578, 2021. [3](#)
- [22] Lawrence Neal, Matthew Olson, Xiaoli Fern, Weng-Keen Wong, and Fuxin Li. Open set learning with counterfactual images. In *Proceedings of the European Conference on Computer Vision (ECCV)*, pages 613–628, 2018. [3](#)
- [23] Walter J Scheirer, Anderson de Rezende Rocha, Archana Sapkota, and Terrance E Boulton. Toward open set recognition. *IEEE transactions on pattern analysis and machine intelligence*, 35(7):1757–1772, 2012. [3](#)
- [24] Patrick Schlachter, Yiwen Liao, and Bin Yang. Open-set recognition using intra-class splitting. In *2019 27th European signal processing conference (EUSIPCO)*, pages 1–5. IEEE, 2019. [3](#)
- [25] Florian Schroff, Dmitry Kalenichenko, and James Philbin. Facenet: A unified embedding for face recognition and clustering. In *2015 IEEE Conference on Computer Vision and Pattern Recognition (CVPR)*, pages 815–823, 2015. [2](#), [3](#)
- [26] Chuanfu Shen, Shiqi Yu, Jilong Wang, George Q Huang, and Liang Wang. A comprehensive survey on deep gait recognition: algorithms, datasets and challenges. *arXiv preprint arXiv:2206.13732*, 2022. [1](#)
- [27] Kohei Shiraga, Yasushi Makihara, Daigo Muramatsu, Tomio Echigo, and Yasushi Yagi. Geinet: View-invariant gait recognition using a convolutional neural network. In *2016 International Conference on Biometrics (ICB)*, pages 1–8, 2016. [1](#), [2](#)
- [28] Noriko Takemura, Yasushi Makihara, Daigo Muramatsu, Tomio Echigo, and Yasushi Yagi. Multi-view large population gait dataset and its performance evaluation for cross-view gait recognition. *IPSJ Transactions on Computer Vision and Applications*, 10(1), 2018. [2](#), [5](#)
- [29] Torben Teepe, Ali Khan, Johannes Gilg, Fabian Herzog, Stefan Hörmann, and Gerhard Rigoll. Gaitgraph: Graph convolutional network for skeleton-based gait recognition. In *2021 IEEE International Conference on Image Processing (ICIP)*, pages 2314–2318. IEEE, 2021. [2](#)
- [30] Sagar Vaze, Kai Han, Andrea Vedaldi, and Andrew Zisserman. Open-set recognition: A good closed-set classifier is all you need? *arXiv preprint arXiv:2110.06207*, 2021. [3](#)

- [31] Ming Wang, Xianda Guo, Beibei Lin, Tian Yang, Zheng Zhu, Lincheng Li, Shunli Zhang, and Xin Yu. Dygait: Exploiting dynamic representations for high-performance gait recognition. *arXiv preprint arXiv:2303.14953*, 2023. 1, 2
- [32] Qian Wu, Ruixuan Xiao, Kaixin Xu, Jingcheng Ni, Boxun Li, and Ziyao Xu. Gaitformer: Revisiting intrinsic periodicity for gait recognition. *arXiv preprint arXiv:2307.13259*, 2023. 2
- [33] Shiqi Yu, Haifeng Chen, Edel B. García Reyes, and Norman Poh. Gaitgan: Invariant gait feature extraction using generative adversarial networks. In *2017 IEEE Conference on Computer Vision and Pattern Recognition Workshops (CVPRW)*, pages 532–539, 2017. 1
- [34] Shiqi Yu, Daoliang Tan, and Tieniu Tan. A framework for evaluating the effect of view angle, clothing and carrying condition on gait recognition. In *18th international conference on pattern recognition (ICPR'06)*, volume 4, pages 441–444. IEEE, 2006. 2, 5
- [35] Jun Zhang, Yong Yan, and Martin Lades. Face recognition: eigenface, elastic matching, and neural nets. *Proceedings of the IEEE*, 85(9):1423–1435, 1997. 4
- [36] Zhilu Zhang and Mert Sabuncu. Generalized cross entropy loss for training deep neural networks with noisy labels. *Advances in neural information processing systems*, 31, 2018. 2, 3
- [37] Guoying Zhao, Guoyi Liu, Hua Li, and Matti Pietikainen. 3d gait recognition using multiple cameras. In *7th International Conference on Automatic Face and Gesture Recognition (FGR06)*, pages 529–534. IEEE, 2006. 2
- [38] Jinkai Zheng, Xinchun Liu, Wu Liu, Lingxiao He, Chenggang Yan, and Tao Mei. Gait recognition in the wild with dense 3d representations and a benchmark. In *Proceedings of the IEEE/CVF Conference on Computer Vision and Pattern Recognition*, pages 20228–20237, 2022. 2, 5
- [39] Zheng Zhu, Xianda Guo, Tian Yang, Junjie Huang, Jiankang Deng, Guan Huang, Dalong Du, Jiwen Lu, and Jie Zhou. Gait recognition in the wild: A benchmark. In *Proceedings of the IEEE/CVF international conference on computer vision*, pages 14789–14799, 2021. 2, 5